iMorpheus.ai

Weekly Journal Club

Loose and Tight GNSS INS Integrations: Comparison of Performance Assessed in Real Urban Scenarios

Friday 26 Jan 2018, 12:00PM

Journal Club

Journal club介绍与自动驾驶中定位方案相关的论文， 主要关注的方向有： SLAM算法、点云数据的处理和压缩、 特征地图、传感器数据处理和融合、 GNSS信号处理等。我们一直关注领域前沿技术， 选取得到广泛认可的、或者是在我们的实际使用中结果比较好的论文， 与大家分享，共同学习成长。

每周五 北京时间12点

http://imorpheus.ai/journalclub

扫码加入无人驾驶技术群

Journal Club

GNSS是许多应用程序和系统定位的主要手段，但是在城市的某些环境中，独立的接收机的性能会出现严重的退化。虽然很多的论文展示了GNSS和INS系统集成的好处，但是他们主要是有高精度的设备和高档IMU。本周介绍的文章主要研究紧耦合集成的性能改进，使用低成本的传感器和大众市场的GNSS，通过在实际城市场景中进行的一系列测试来对其性能进行评估。

每周五 北京时间12点
http://imorpheus.ai/journalclub

扫码加入无人驾驶技术群

Gianluca Falco *, Marco Pini and Gianluca Marucco
Istituto Superiore Mario Boella, Torino 10138, Italy;

Outlines

1. Introduction to Navigation Algorithms Based on GNSS/INS Integrations
2. Performance Assessment in Real Urban Scenarios
3. Results of Tests
4. Conclusion

iMorpheus.ai

1. Navigation Algorithms Based on Global Navigation Satellite System (GNSS)/Inertial Navigation Systems (INS) Integrations

1.1. Common Loosely-Coupled Architecture

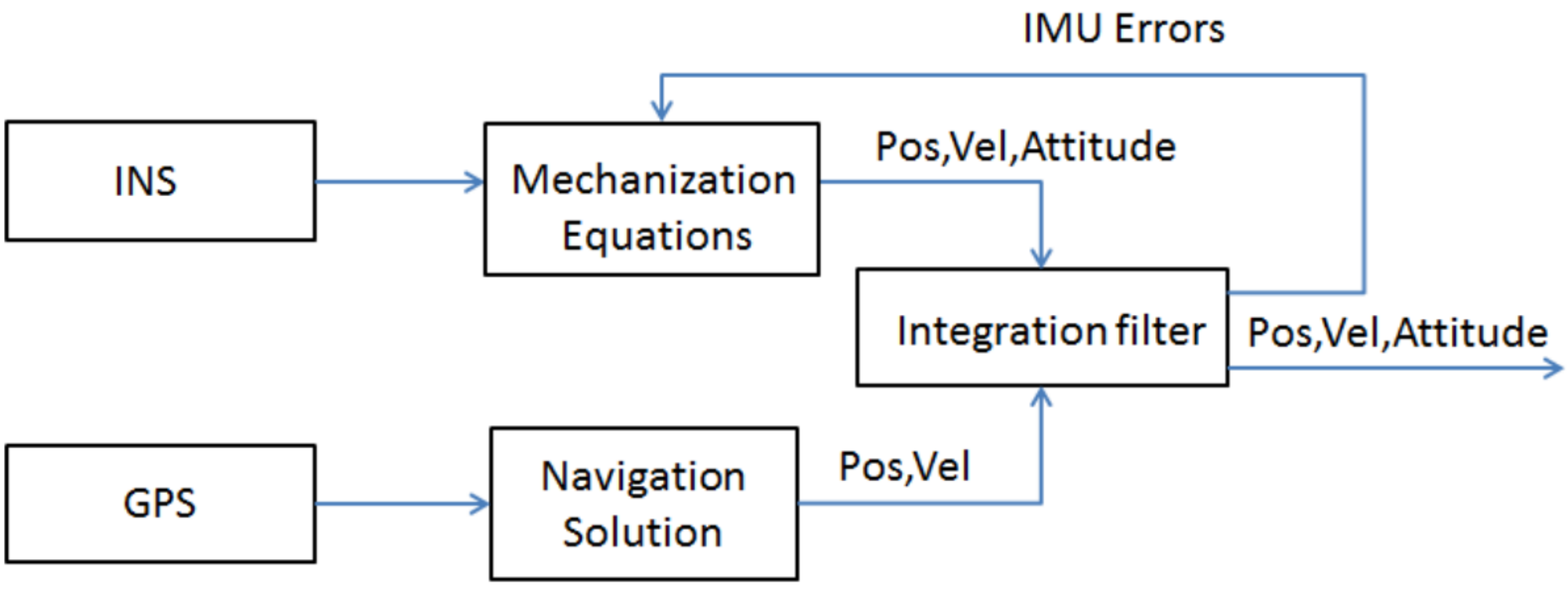

Figure 1. Block diagram of a common loosely-coupled architecture.

1.2. Common Tightly-Coupled Architecture

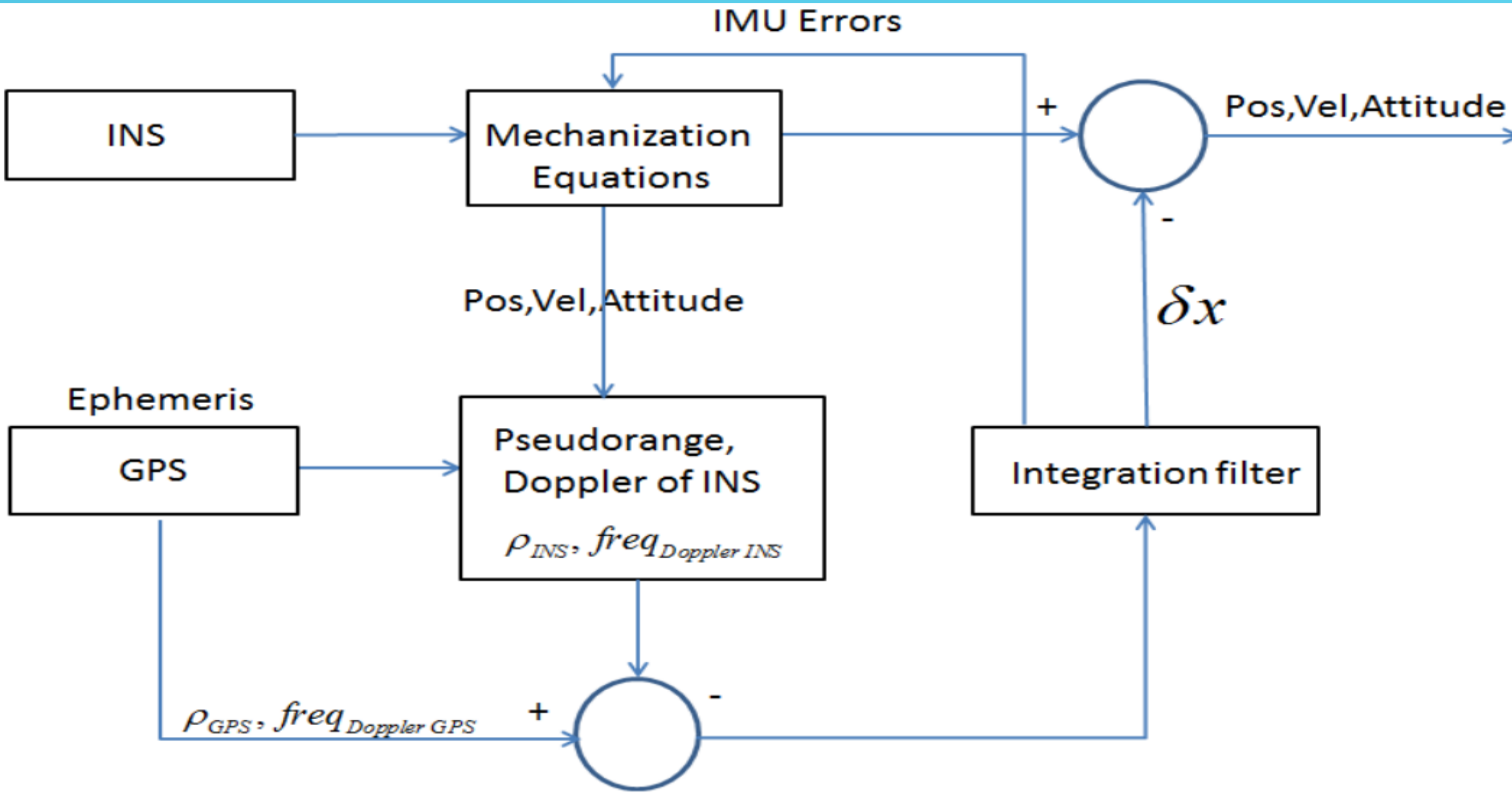

Figure 2. Block diagram of a common tightly-coupled architecture.

Considering an ECEF-frame navigation, the error states estimated by the GNSS/INS integration Kalman filter can be written as:

$$\delta x = \left[\underbrace{\delta x\,\delta y\,\delta z}_{\delta r}\ \underbrace{\delta V_x\,\delta V_y\,\delta V_z}_{\delta v}\ \underbrace{\delta A_x\,\delta A_y\,\delta A_z}_{\delta A}\ \underbrace{\delta\omega_x\,\delta\omega_y\,\delta\omega_z}_{\delta\omega}\ \underbrace{\delta f_x\,\delta f_y\,\delta f_z}_{\delta f}\ \underbrace{\delta t\,\delta t'}_{\delta b} \right]$$

The discrete transition matrix Φk expressed in ECEF-frame, can be written as:

$$\Phi_k = \begin{bmatrix} I_{3\times3} & T_k \cdot I_{3\times3} & 0_{3\times3} & 0_{3\times3} & 0_{3\times3} & 0 & 0 \\ N^e & I_{3\times3} - 2T_k\Omega_{ie}^e & -T_kF_k & 0_{3\times3} & T_kC_{b,k3\times3}^e & 0 & 0 \\ 0_{3\times3} & 0_{3\times3} & I_{3\times3} - T_k\Omega_{ie}^e & T_kC_{b,k}^e & 0_{3\times3} & 0 & 0 \\ 0_{3\times3} & 0_{3\times3} & 0_{3\times3} & I_{3x3} + T_kD_g & 0_{3\times3} & 0 & 0 \\ 0_{3\times3} & 0_{3\times3} & 0_{3\times3} & 0_{3\times3} & I_{3\times3} + T_kD_a & 0 & 0 \\ 0_{1\times3} & 0_{1\times3} & 0_{1\times3} & 0_{1\times3} & 0_{1\times3} & 0 & 1 \\ 0_{1\times3} & 0_{1\times3} & 0_{1\times3} & 0_{1\times3} & 0_{1\times3} & 0 & 0 \end{bmatrix}$$

iMorpheus.ai

In order to take into account how the noise affecting the INS sensors is distributed among the state vectors parameter, can be written as:

$$\delta x_k = \Phi_{k-1}\delta x_{k-1} + G_{k-1}\omega_{k-1}$$

The definition of the model noise vector µk is reported in (8):

$$\mu_k = \left[\mu_{t,k}, (\mu_{a,k})^{\mathrm{T}}, \left(\mu_{g,k}\right)^{\mathrm{T}}, \mu_{t',k}, (\mu_{aa,k})^{\mathrm{T}}, \left(\mu_{gg,k}\right)^{\mathrm{T}}\right]^{\mathrm{T}} \quad \mu_k \in \Re^{14,1}$$

iMorpheus.ai

1.3. Designed Tightly-Coupled Architecture

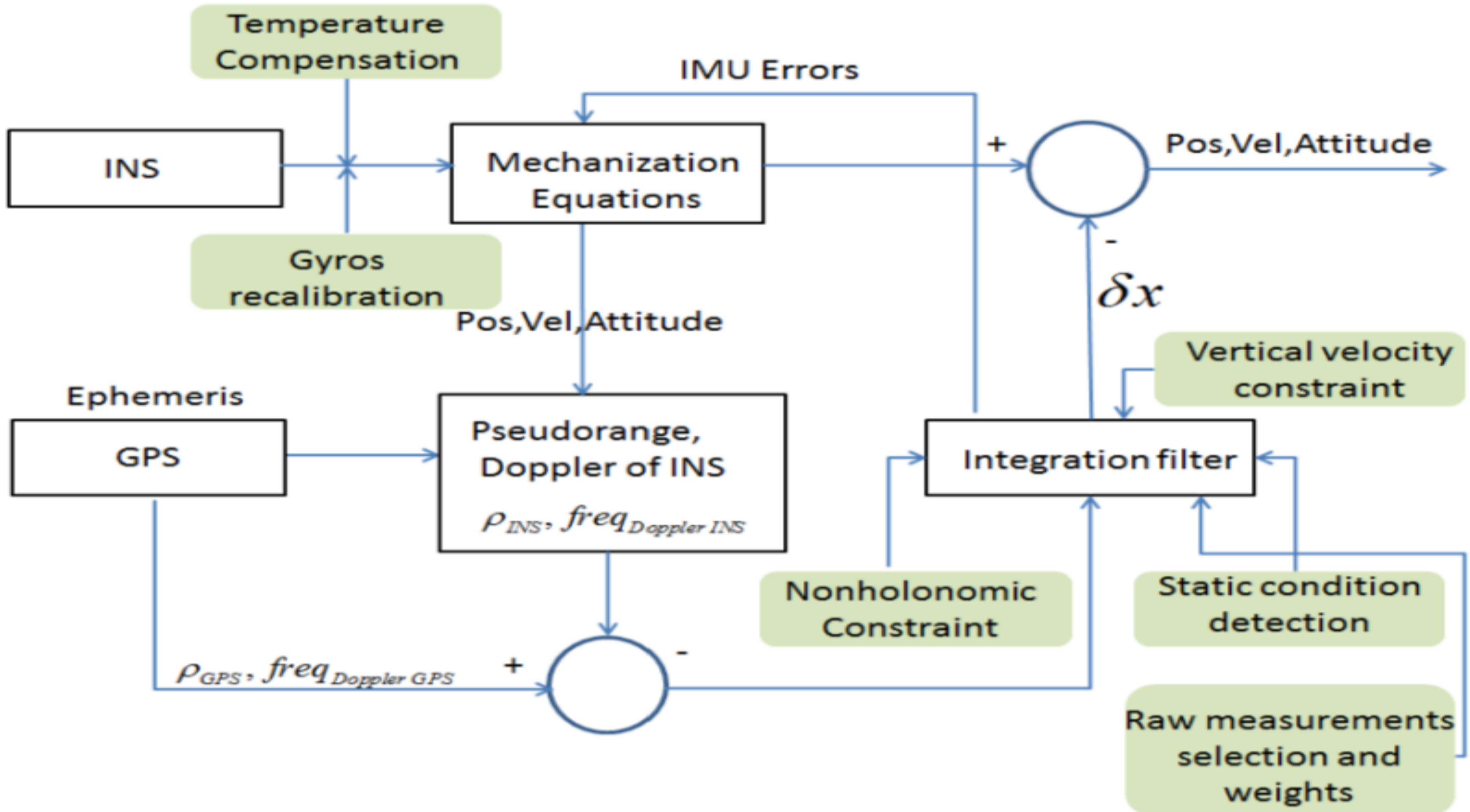

Figure 3. Block diagram of a designed tightly-coupled architecture.

1.3.1. Temperature Compensation

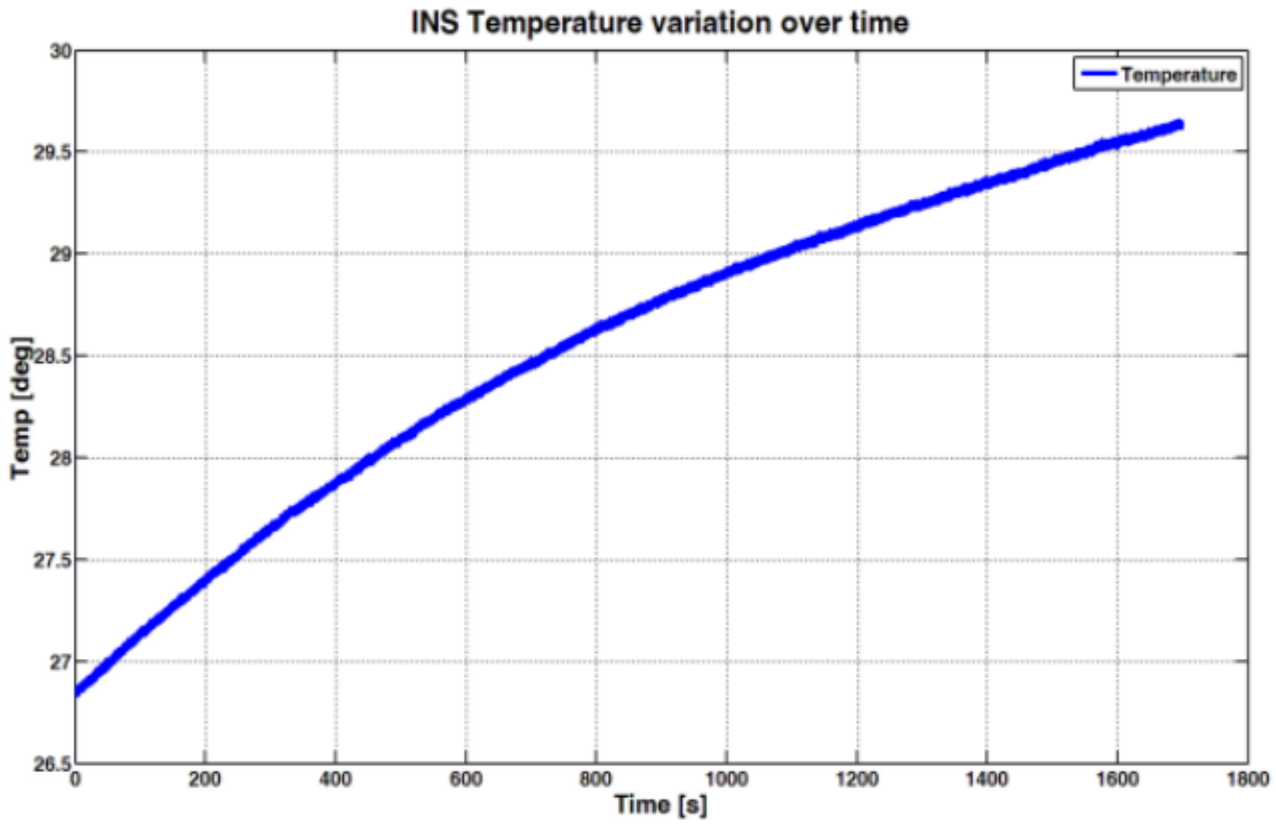

(a)

iMorpheus.ai

1.3.1. Temperature Compensation

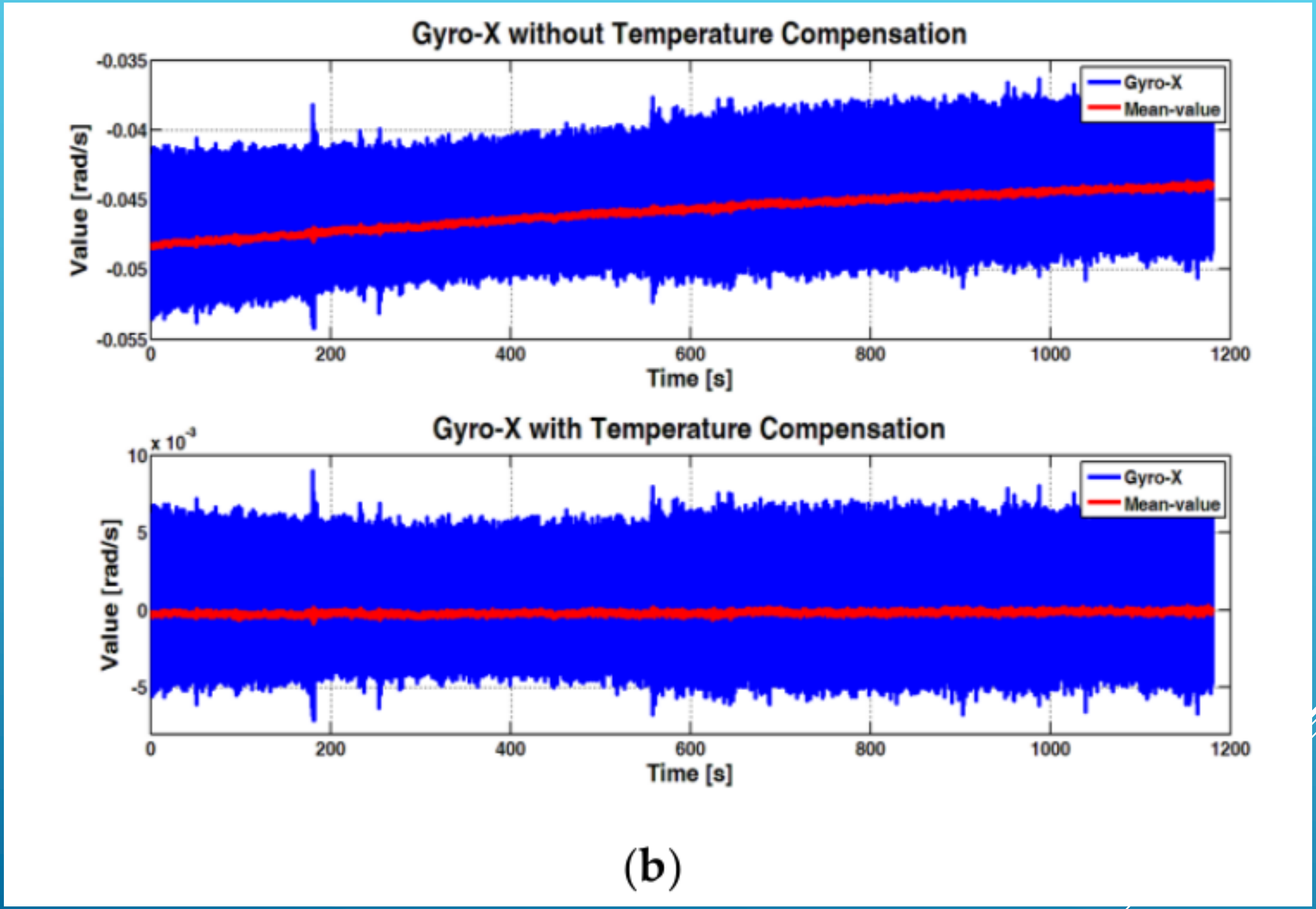

In our design, we estimated the INS sensors biases off-line, installing the IMU into a temperature-controlled chamber and rotating the IMU in different positions. We repeated the same procedure for different temperatures in the range –20 to 60 ◦C.

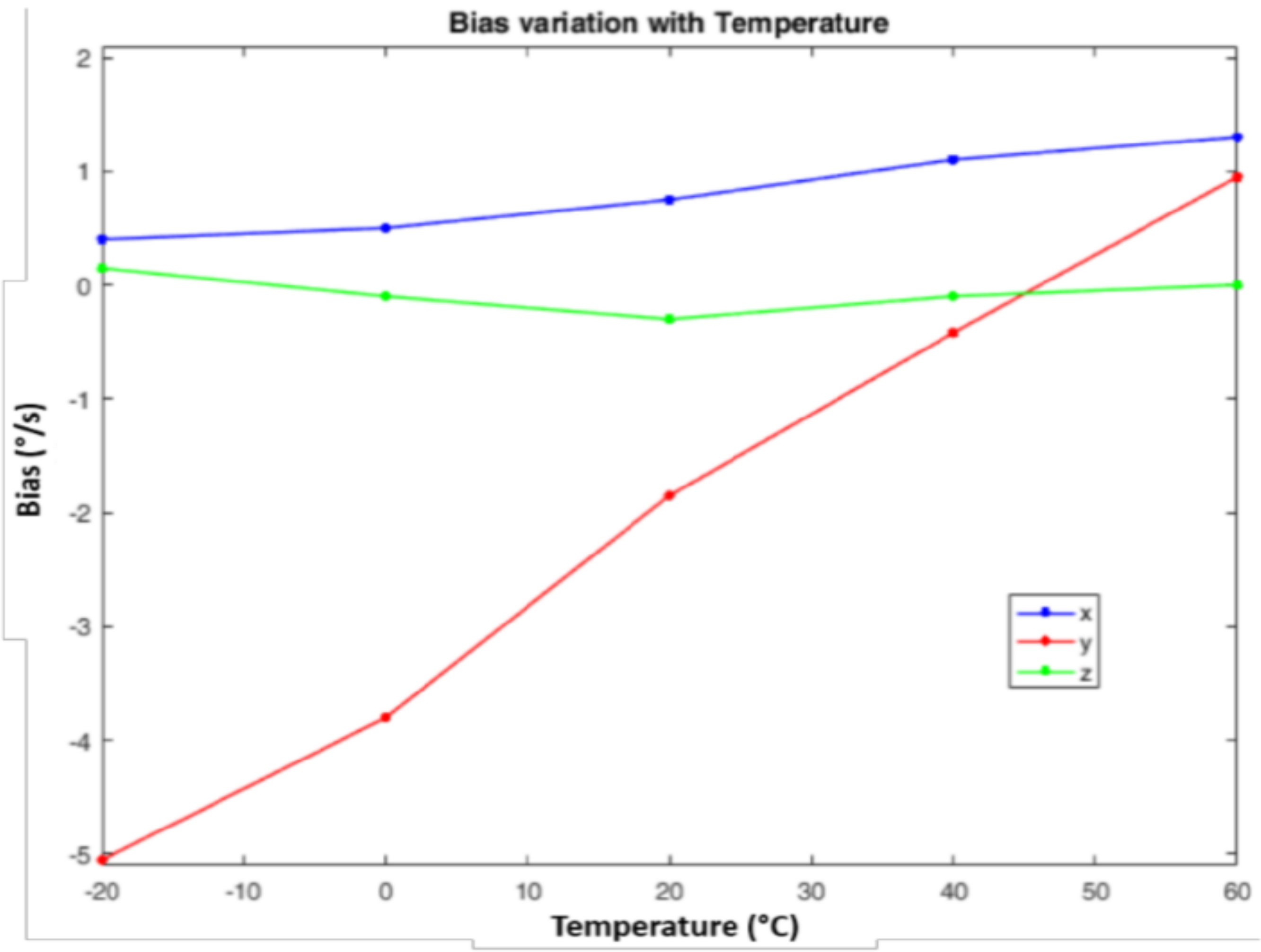

Figure 5. InvenSense MPU Gyros Bias vs. Temperature.

iMorpheus.ai

1.3.2. Gyros Recalibration

1.3.3. Static Condition Detection

1.3.4. Nonholonomic Constraints

1.3.5. Vertical Velocity Constraint

1.3.6. Raw Measurement Selection and Weights

iMorpheus.ai

2. Performance Assessment in Real Urban Scenarios

This section describes the urban scenarios selected for the experimental tests and presents the metrics used to assess the algorithms' performances.

Figure 6. Trajectory followed during the experimental tests in Turin.

Zone 1, that is a car parking area, characterized by good visibility of the sky;

Zone 2, that is characterized by narrow streets and densely packed buildings, limiting the number of satellites in view. Moreover, in that part of the trajectory, the vehicle is expected to experience frequent stops and sharp turns;

Zone 3, that is a straight avenue of trees, surrounded by buildings that likely generate multipath degrading the received GNSS signals.

iMorpheus.ai

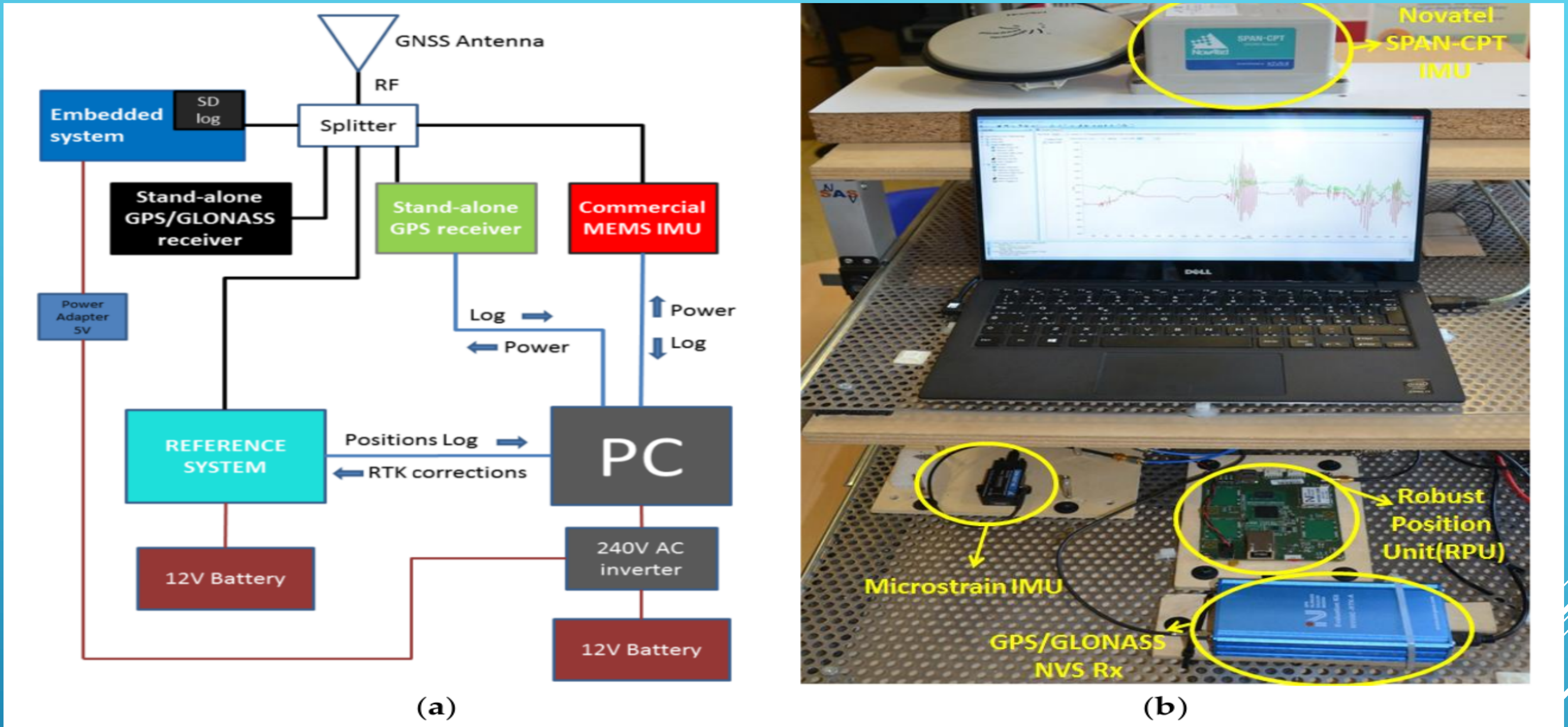

Figure 7. Setup (**a**) and the setup mounted on board mounted on board of a car (**b**).

Table 1. Hardware components and navigation technique used during the tests.

Label	Hardware	Navigation Technique
Tight	Embedded System	GPS+INS tightly-coupled algorithm
Microstrain	Commercial MEMS IMU (i.e., Microstrain 3DM-Gx3-45)	GPS+INS loosely-coupled algorithm
GPS Rx	Standalone GPS receiver (i.e., NVS NV08C-CSM)	Standalone GPS PVT solution
GPS+GLONASS Rx	Standalone GPS/GLONASS receiver (i.e., NVS NV08C-CSM)	Standalone GPS+GLONASS PVT solution
Ref NOVATEL	REFERENCE SYSTEM (i.e., Novatel SPAN-CPT)	Dual Frequency GPS, RTK+INS tightly-coupled algorithm

3. Results of Tests

3.1. Zone 1: Car Parking Area

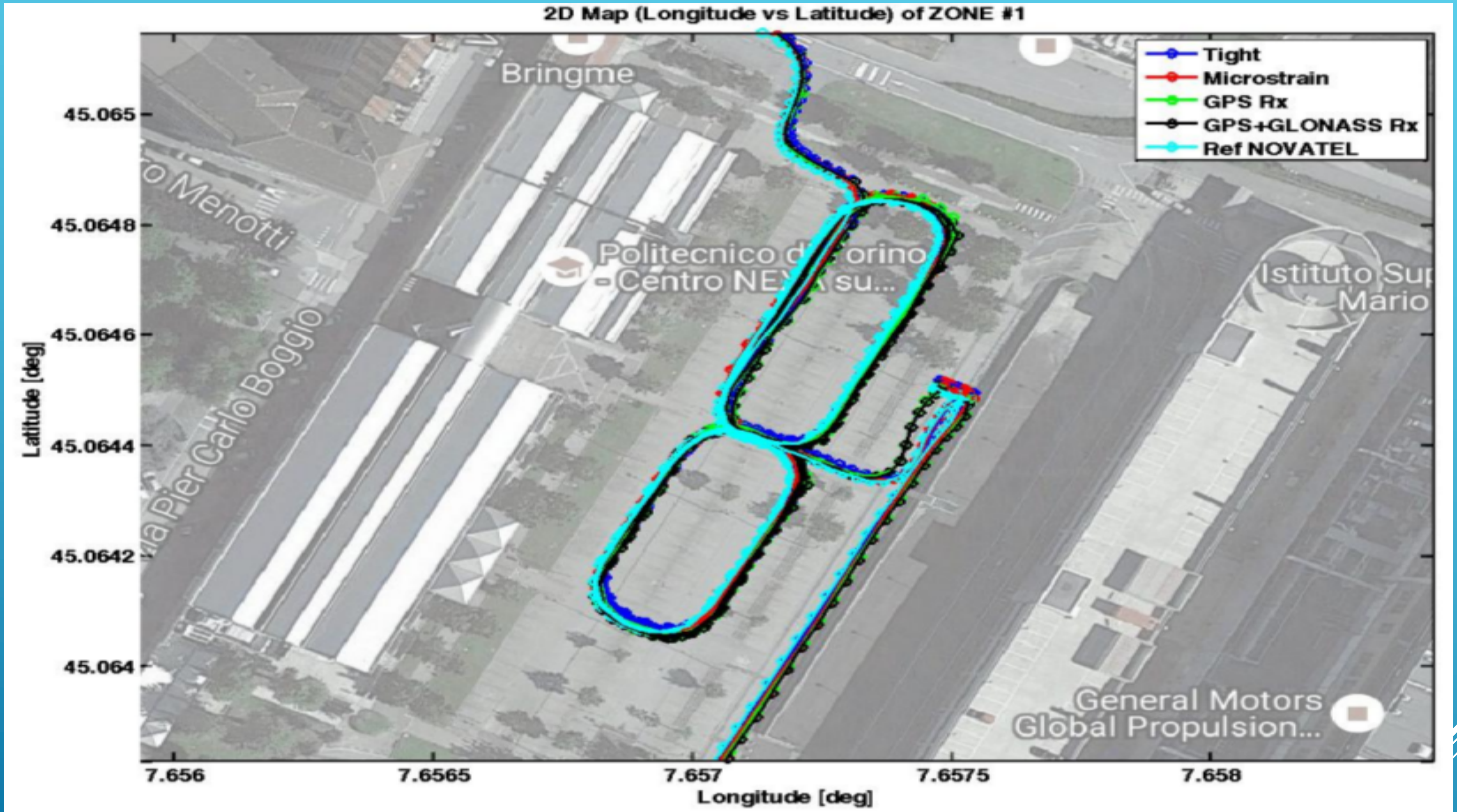

Figure 8. Trajectories collected by the devices being tested in Zone 1.

HPE

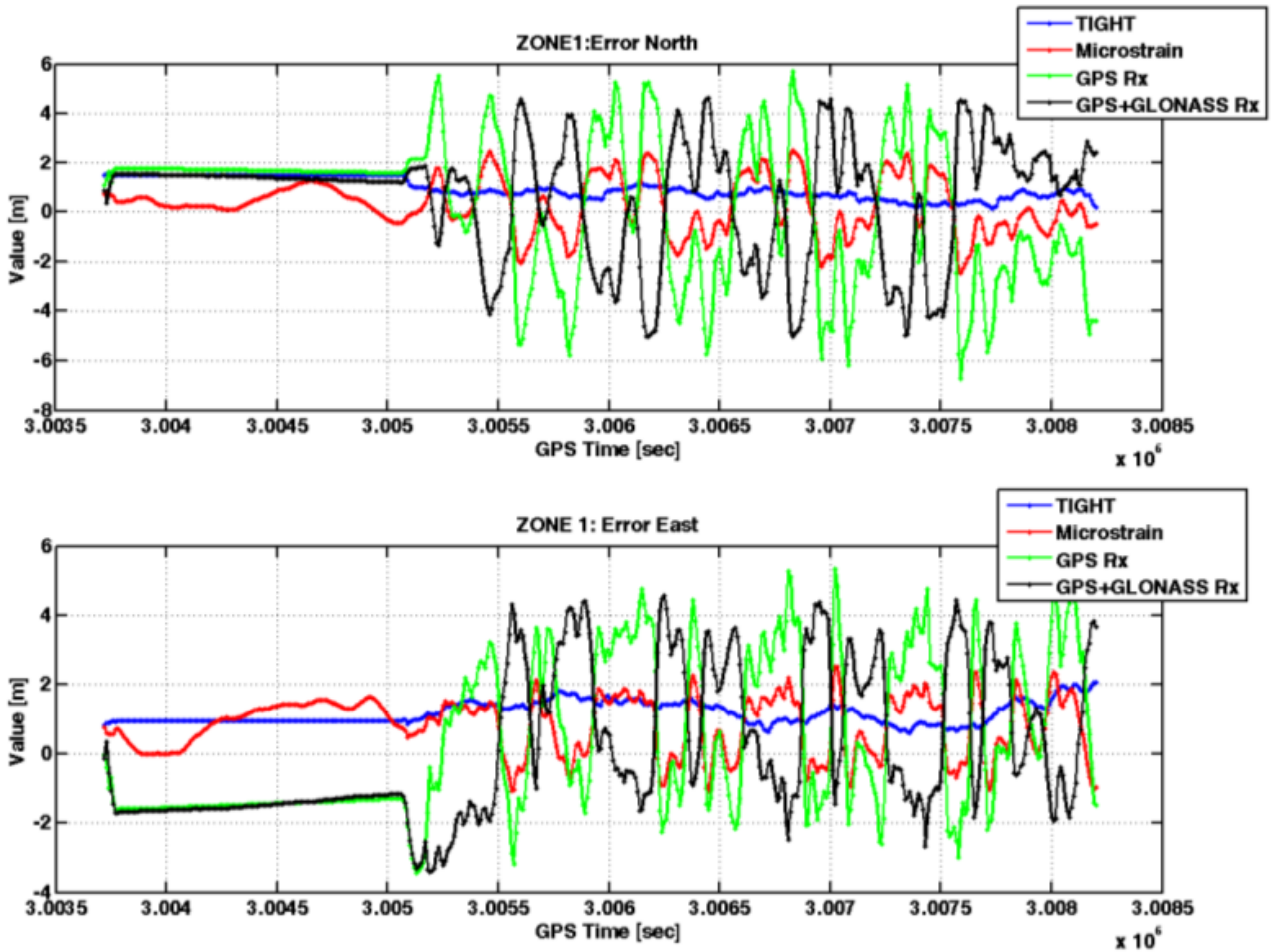
ZONE1:Error North
TIGHT
Microstrain
GPS Rx
GPS+GLONASS Rx
Value [m]
GPS Time [sec]
x 10^6
6
4
2
0
-2
-4
-6
-8
3.0035
3.004
3.0045
3.005
3.0055
3.006
3.0065
3.007
3.0075
3.008
3.0085
ZONE 1: Error East
TIGHT
Microstrain
GPS Rx
GPS+GLONASS Rx
Value [m]
GPS Time [sec]
x 10^6
6
4
2
0
-2
-4
3.0035
3.004
3.0045
3.005
3.0055
3.006
3.0065
3.007
3.0075
3.008
3.0085

(a)

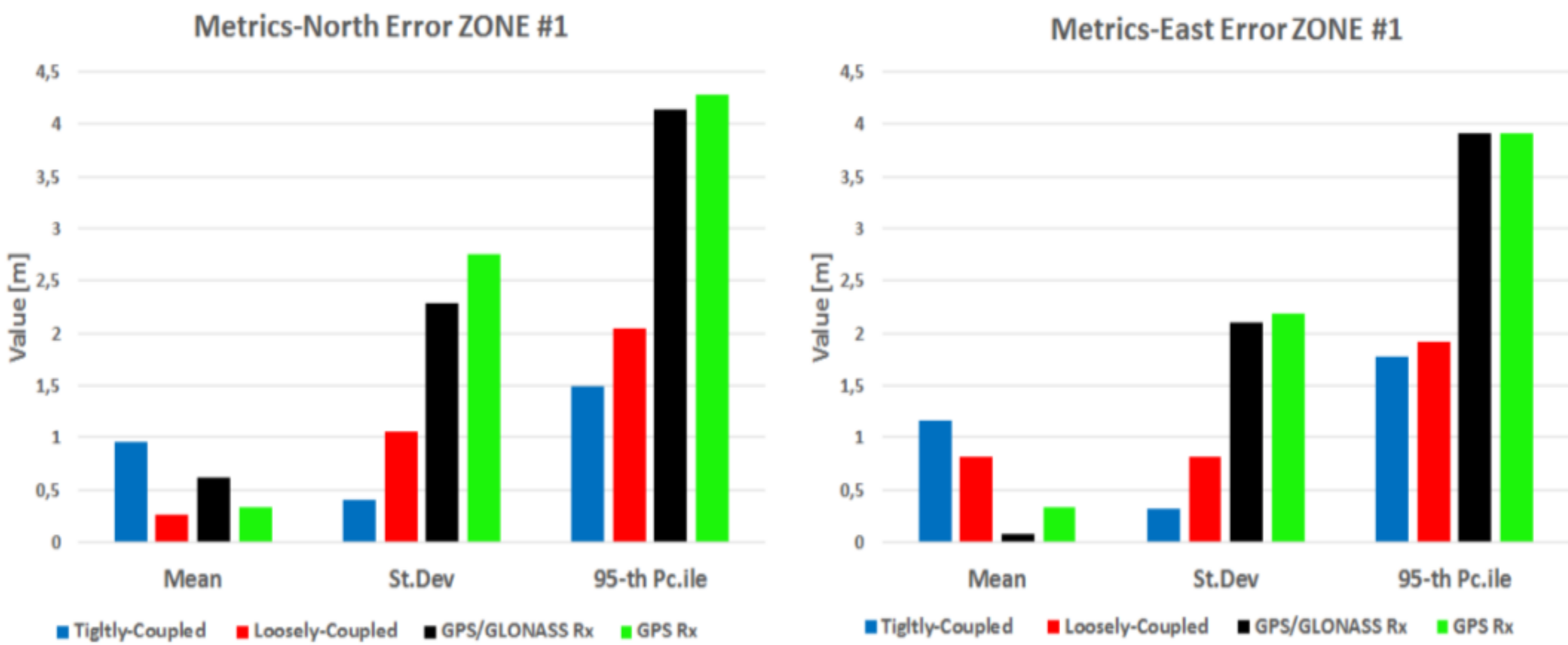

Metrics-North Error ZONE #1
Value [m]
4,5
4
3,5
3
2,5
2
1,5
1
0,5
0
Mean
St.Dev
95-th Pc.ile
Tigltly-Coupled
Loosely-Coupled
GPS/GLONASS Rx
GPS Rx
Metrics-East Error ZONE #1
Value [m]
4,5
4
3,5
3
2,5
2
1,5
1
0,5
0
Mean
St.Dev
95-th Pc.ile
Tigltly-Coupled
Loosely-Coupled
GPS/GLONASS Rx
GPS Rx

(b)

Figure 10 shows the yaw angles estimated by the embedded system running the tightly-coupled algorithm (blue line) and those obtained by the commercial MEMS IMU (red line). The figure also plots in cyan the yaw angles estimated by the reference receiver.

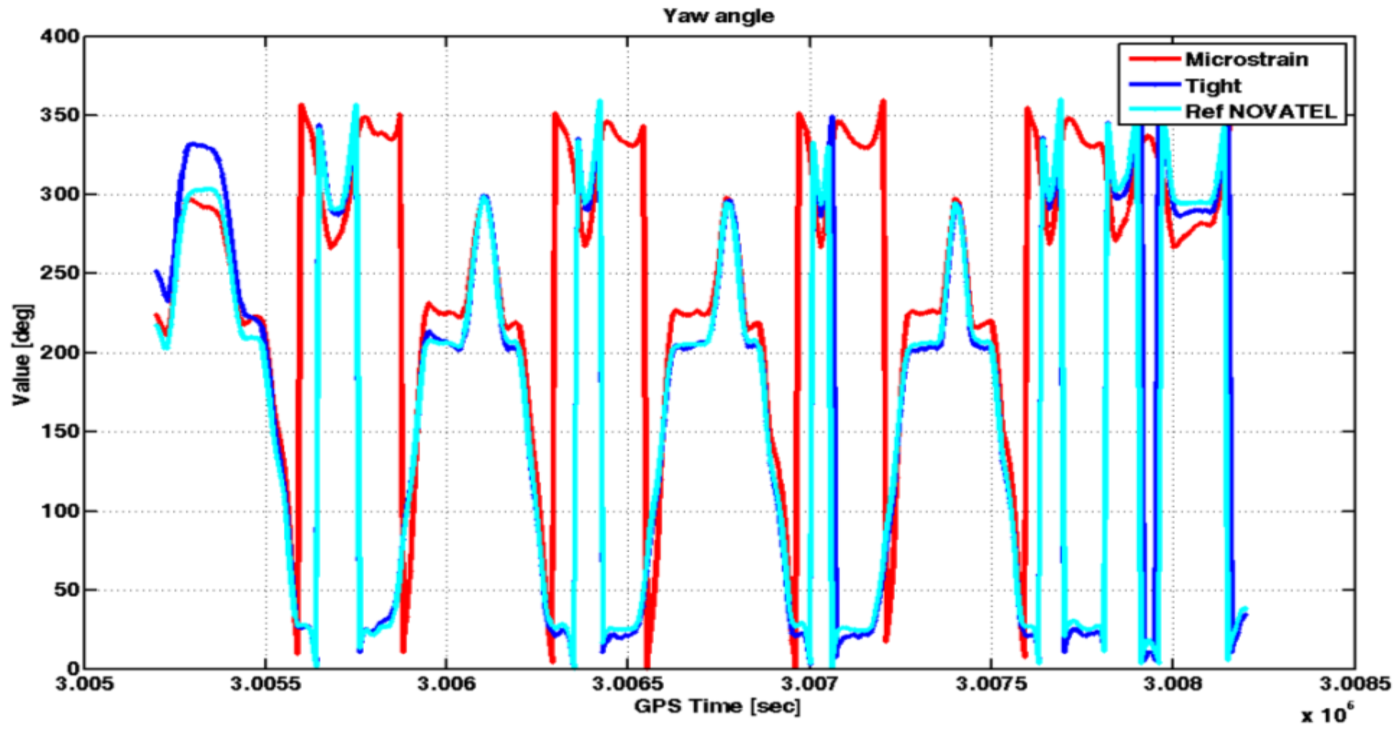

Figure 10. Yaw angles estimated by different MEMS IMU sensors under investigation in the Zone 1.

3.2. Zone 2: Urban Canyon

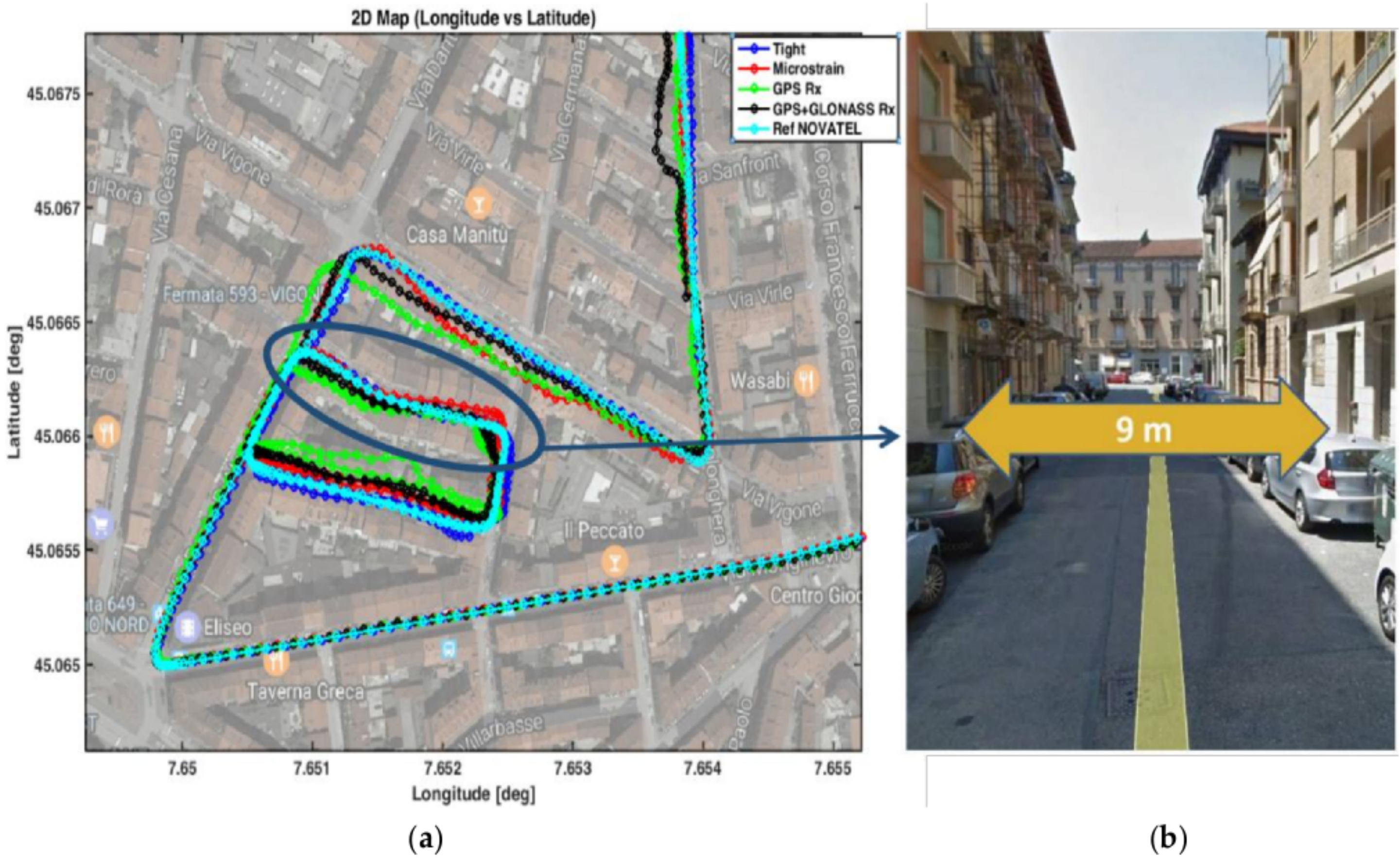

Figure 12. Trajectories collected by the devices being tested in Zone 2 (**a**) and picture of a narrow street passed through during the test (**b**).

HPE

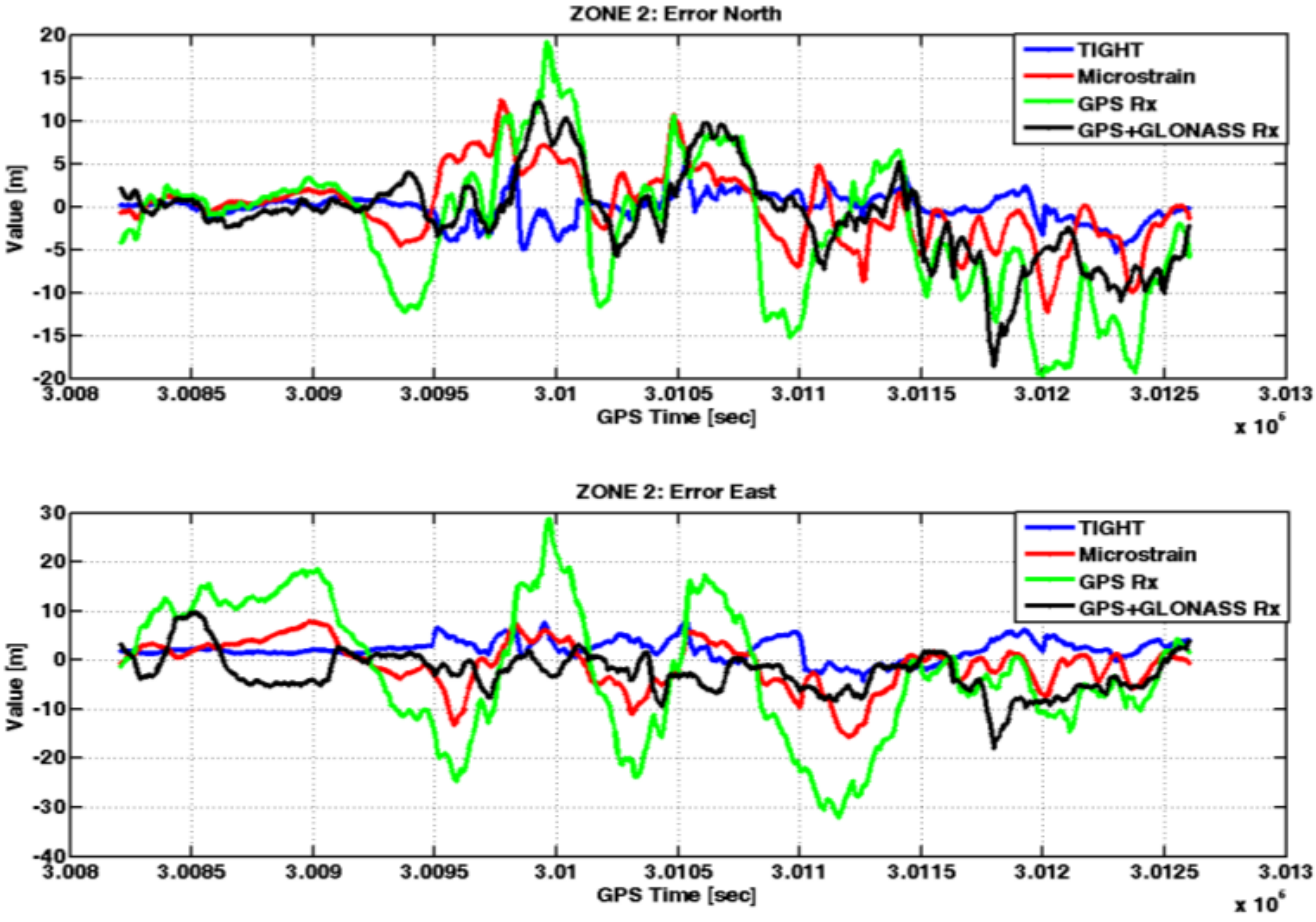
ZONE 2: Error North
Value [m]
GPS Time [sec]
x 10^6
TIGHT
Microstrain
GPS Rx
GPS+GLONASS Rx
ZONE 2: Error East
Value [m]
GPS Time [sec]
x 10^6
TIGHT
Microstrain
GPS Rx
GPS+GLONASS Rx

(a)

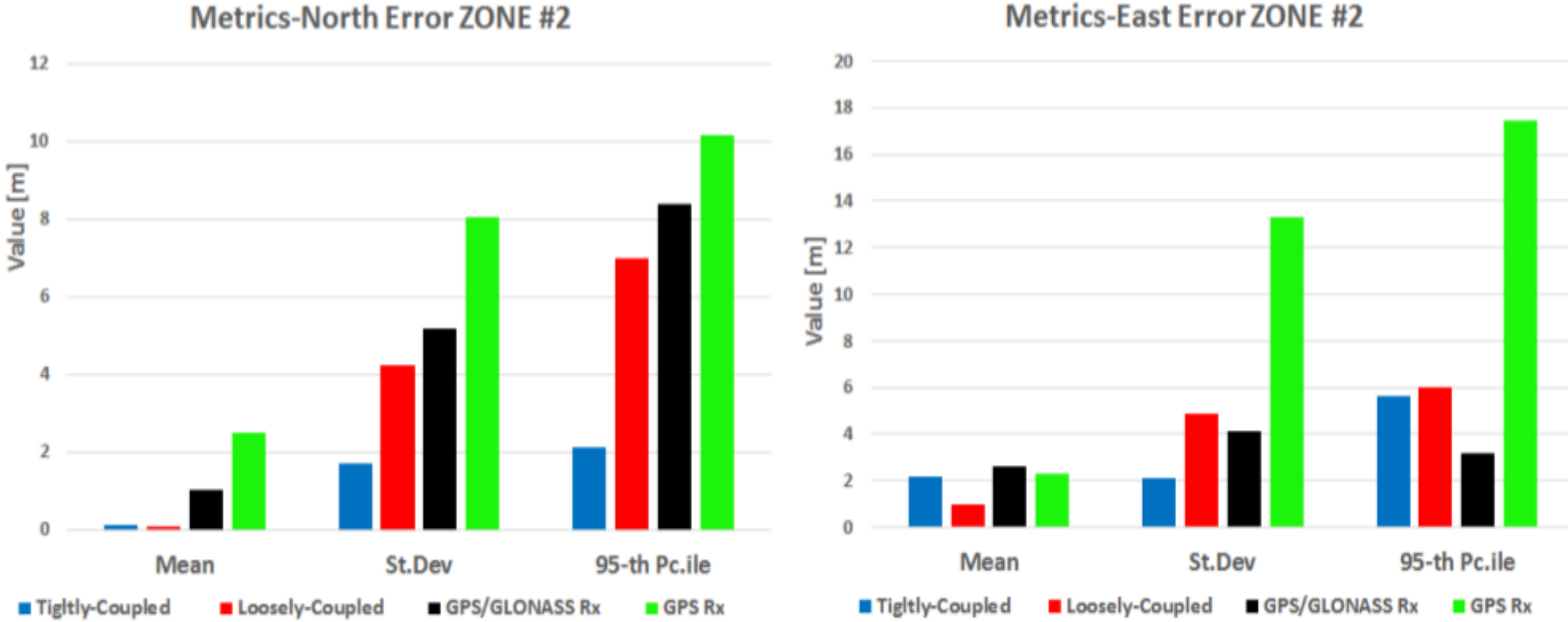

(b)

iMorpheus.ai

Figure 14 shows the yaw angle estimated by the embedded system running the tightly-coupled algorithm and the commercial MEMS IMU.

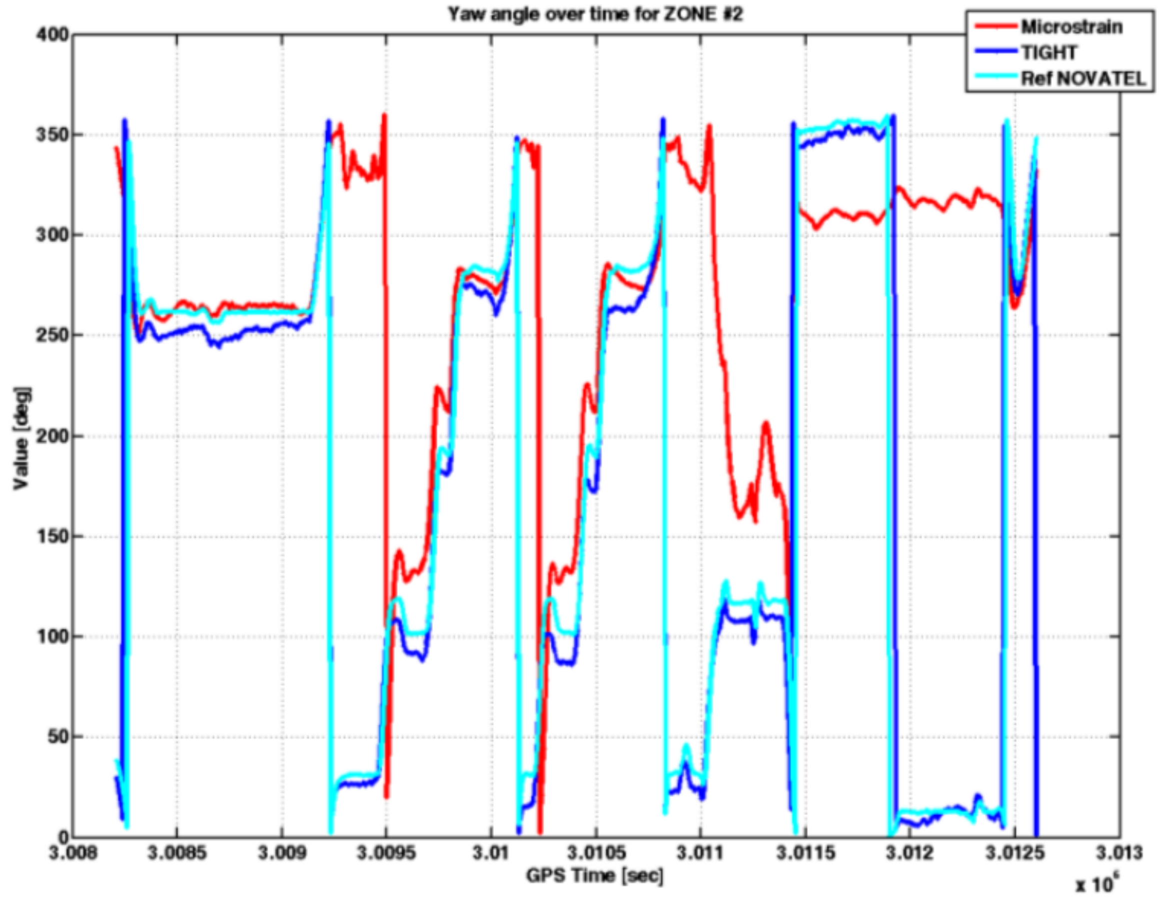

Figure 14. Yaw angles estimated by different MEMS IMU sensors under investigation in Zone 2.

4.3.Zone 3: Straight Avenue of Trees

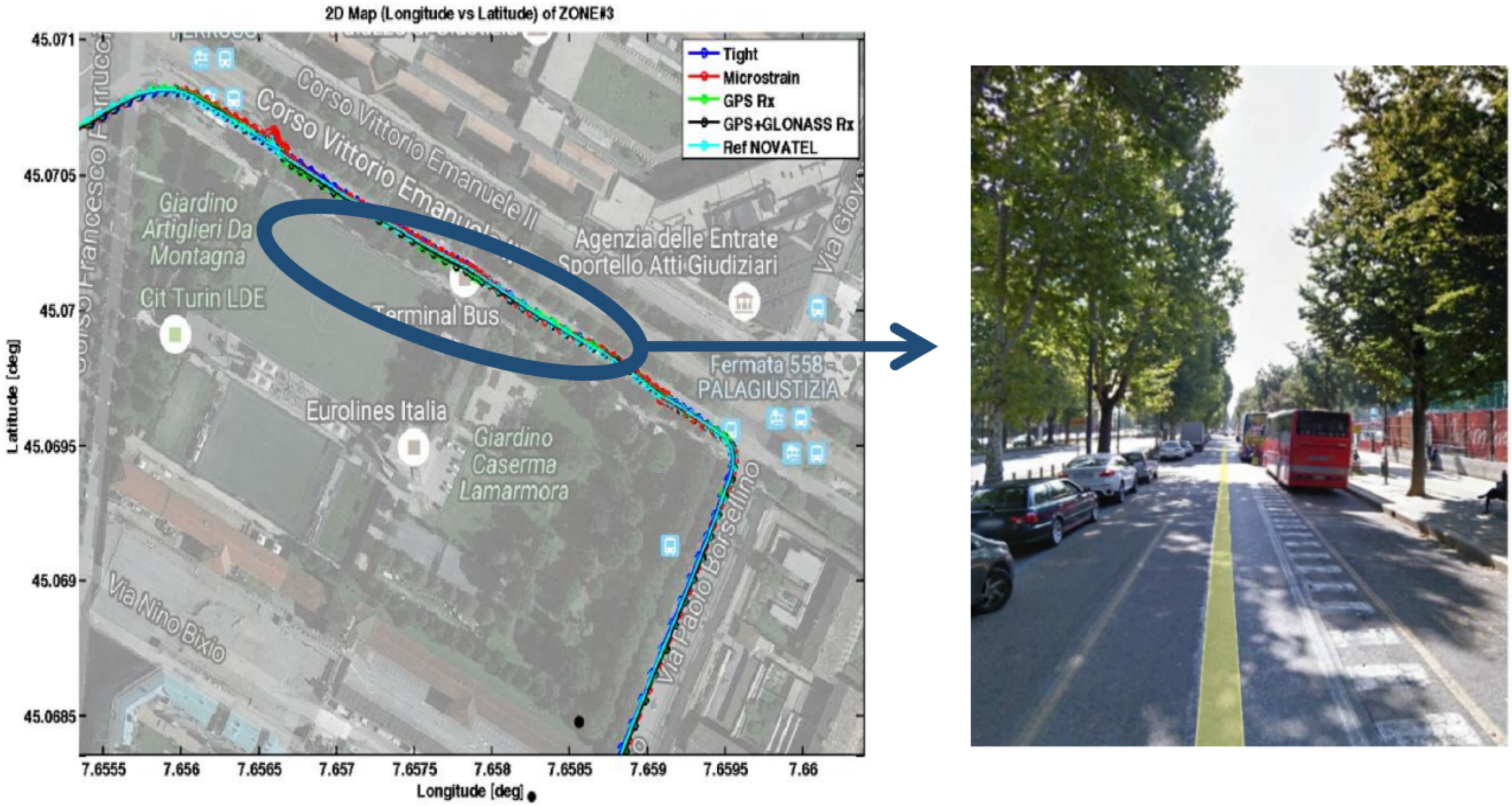

(a) (b)

Figure 16. Trajectories collected by the devices being tested in Zone 3 (**a**). A tree-lined street is depicted in (**b**).

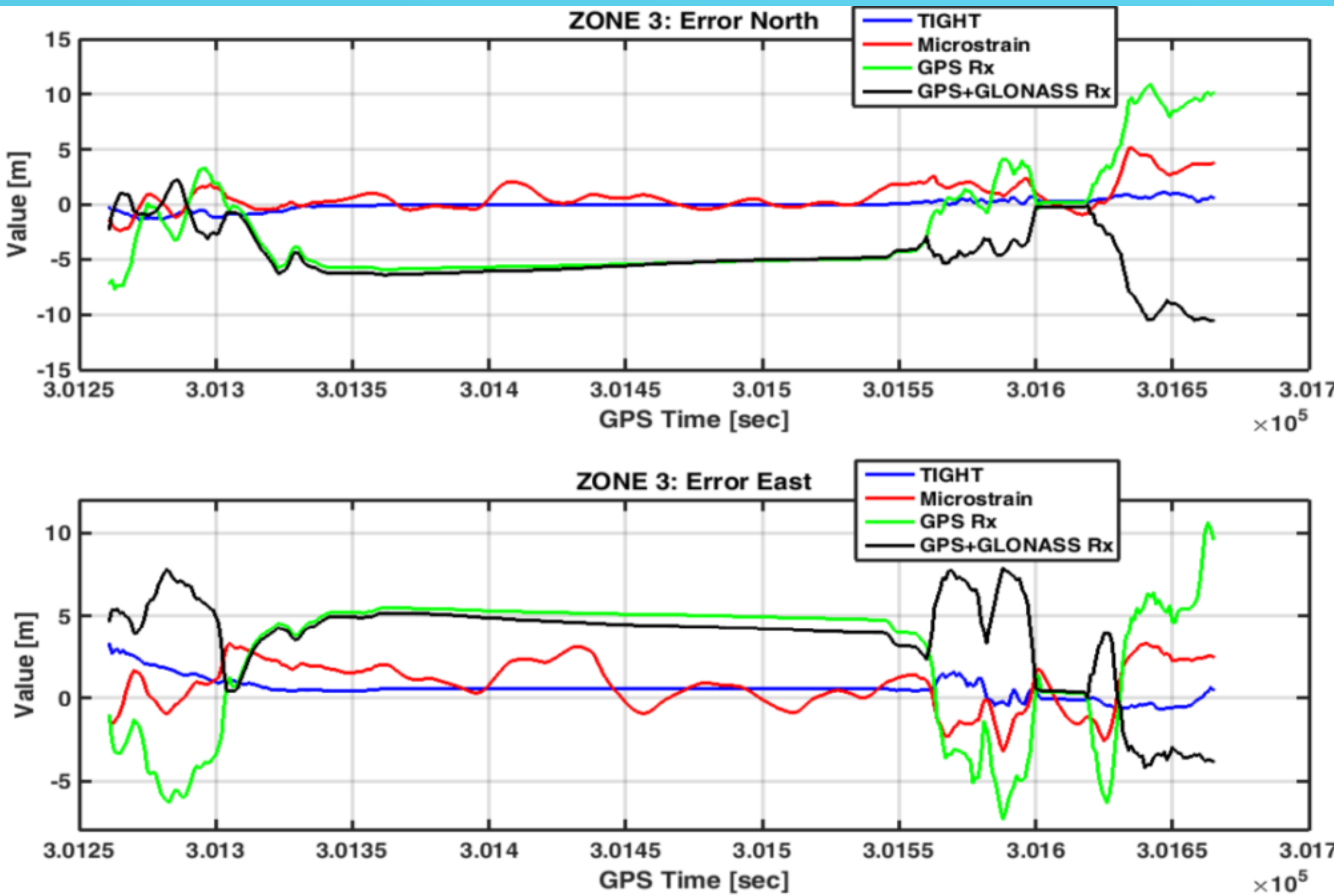

ZONE 3: Error North
TIGHT
Microstrain
GPS Rx
GPS+GLONASS Rx
Value [m]
15
10
5
0
-5
-10
-15
3.0125
3.013
3.0135
3.014
3.0145
3.015
3.0155
3.016
3.0165
3.017
GPS Time [sec]
×10^5
ZONE 3: Error East
TIGHT
Microstrain
GPS Rx
GPS+GLONASS Rx
Value [m]
10
5
0
-5
3.0125
3.013
3.0135
3.014
3.0145
3.015
3.0155
3.016
3.0165
3.017
GPS Time [sec]
×10^5

(a)

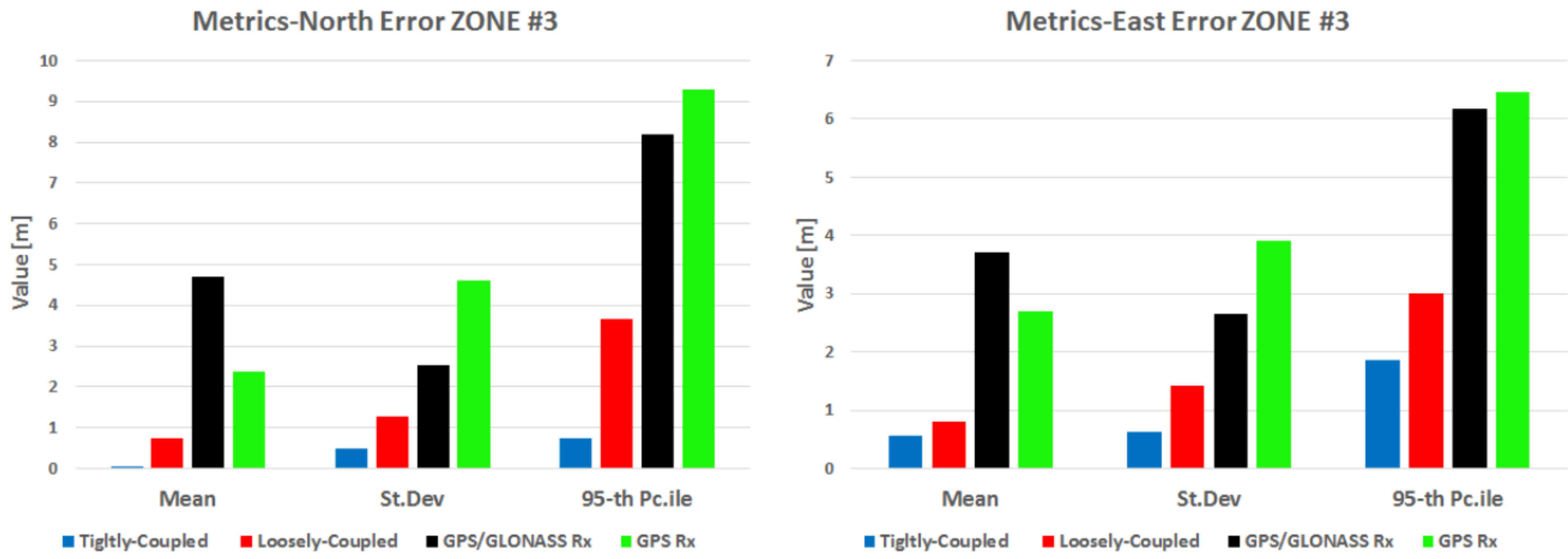

(b)

iMorpheus.ai

Figure 18 shows the yaw angle estimated by the embedded system running the tightly-coupled algorithm and the commercial MEMS IMU.

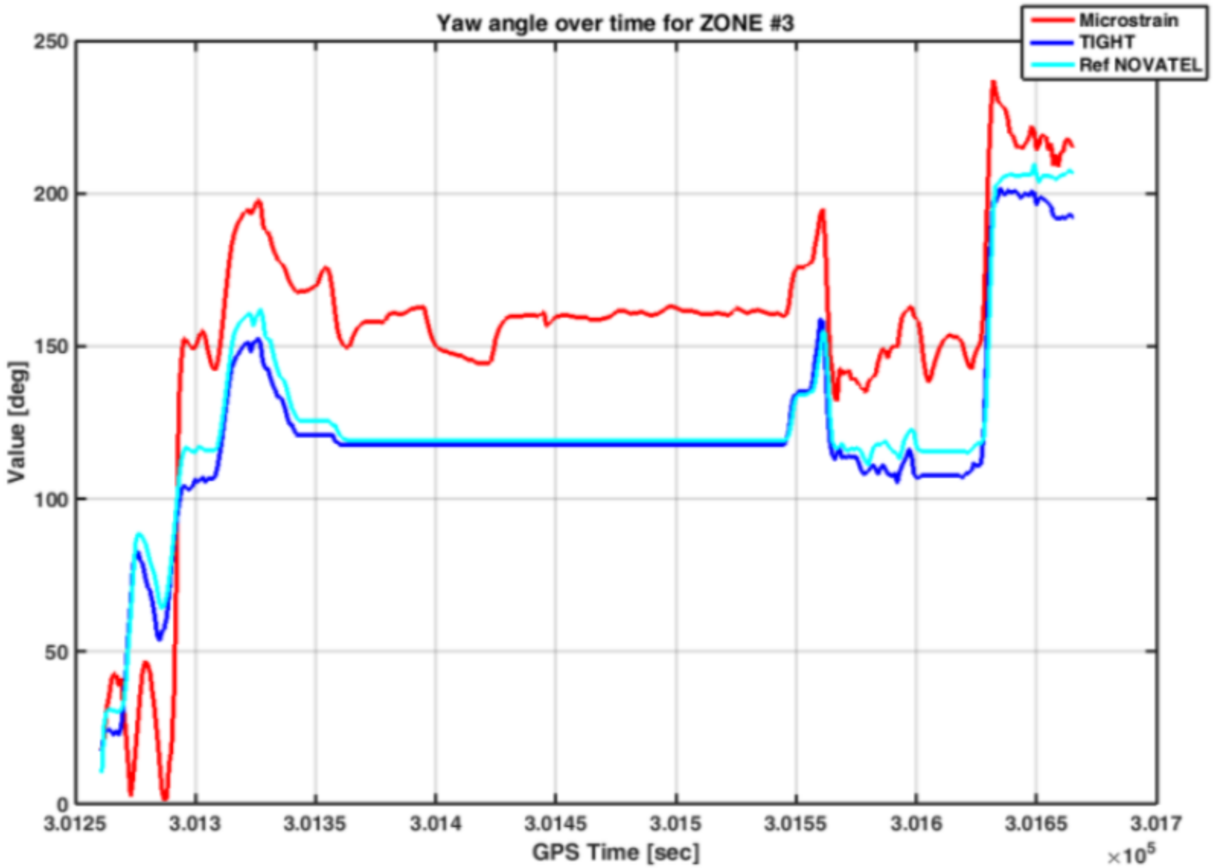

Figure 18. Yaw angles estimated by different MEMS IMU sensors under investigation in Zone 3.

4. Conclusions

This paper presents the assessment of the positioning performance of a GNSS/INS tightly-coupled algorithm, measured in real urban scenarios. The algorithm was designed to fuse measurements from a low-cost INS and a mass-market Global Positioning System (GPS) receiver. Results show a significant decrement of the positioning errors, if compared to those obtained with other commercial devices. In particular, the tightly-coupled algorithm provides better estimates of the vehicle position and attitude, with respect to a commercial GPS module, loosely integrated with an inertial sensor. The improvement was measured following a standardized testing method, considering the horizontal position error and the yaw angle, as the main performance metrics. The experimental results reported in this paper demonstrate the possibility to employ tightly-coupled architectures also in mass-market devices, often employed in applications where users move in urban spaces. In the years ahead, the improvement of Micro Electrical Mechanical Sensors (MEMS) technology and the evolution of GNSS, with enhanced signal formats, different frequency bands and more satellites in view, are expected to further increase the positioning performance of mass-market devices, enabling a variety of new services for road users.

iMorpheus.ai

JC

Journal Club

iMorpheus.ai Weekly Journal Club

Next Friday, 02/02/2018 12:00PM GMT+8

An Introduction to the Kalman Filter

Website : **http://imorpheus.ai**

Email Address : **live@imorpheus.ai**

iMorpheus.ai